

Preparation and Characterization of Mesoporous Zirconia Made by Using a Poly (methyl methacrylate) Template

Guorong Duan · Chunxiang Zhang ·
Aimei Li · Xujie Yang · Lude Lu · Xin Wang

Received: 29 November 2007 / Accepted: 14 February 2008 / Published online: 28 February 2008
© to the authors 2008

Abstract Superfine powders of poly (methyl methacrylate) (PMMA) have been prepared by means of an emulsion polymerization method. These have been used as templates in the synthesis of tetragonal phase mesoporous zirconia by the sol–gel method, using zirconium oxychloride and oxalic acid as raw materials. The products have been characterized by infrared spectroscopy, X-ray diffraction analysis, transmission electron microscopy, N_2 adsorption-desorption isotherms, and pore size distribution. The results indicate that the average pore size was found to be 3.7 nm.

Keywords Zirconia · Mesoporous · PMMA · Sol–gel · Template

Introduction

Due to their large surface areas, controllable pore size, and easy functionalization [1], mesoporous materials have opened many new possibilities for applications in catalysis, as catalyst supports, in separation science, and in drug delivery, as well as for protein encapsulation. Over the past few decades, preparation techniques for mesoporous structures have attracted the attention of many researchers [2–4]. Most research in this field has been focused on silica as a framework structure [5, 6]. However, mesoporous

materials derived from transition metal oxides rather than silica frameworks are expected to be quite useful for several applications [7, 8]. At present, stabilized t-ZrO₂ at room temperature is considered to be an important structural ceramic because of its excellent mechanical properties, such as fracture toughness, high strength, and hardness [9, 10], and there have been several reports concerning the synthesis of mesoporous structures [11]. However, synthetic mesoporous zirconia has poor structural stability [12]. One difficulty stems from a facile crystallization of zirconia, which is accompanied by structural collapse, during formation of the mesoporous phase and removal of the template [13–15]. A further difficulty is the phase transformation of zirconia from tetragonal phase to monoclinic phase when the products are cooled down from high temperature to ambient conditions [16, 17]. The resulting defects will affect the potential applications of the mesoporous zirconia.

In this work, we have used the inexpensive inorganic material zirconium oxychloride and oxalic acid as raw materials to prepare mesoporous zirconia by a sol–gel method [18] with the aid of PMMA as a template. Importantly, the space occupied by the PMMA particles shrinks from the micron or submicron size range to the nanosized range as a result of the structural collapse that accompanies the crystallization of zirconia.

Experimental

Materials

Methyl methacrylate (MMA) and sodium dodecyl sulfate (SDS), both of chemical reagent grade, were purchased from Shanghai Lingfeng Chemistry Co. Ltd., China;

G. Duan (✉) · A. Li
Ruidi Engineering & Technology Center, Nanjing Hydraulic
Research Institute, Nanjing 210024, P.R. China
e-mail: duangr2003@yahoo.com.cn

G. Duan · C. Zhang · X. Yang · L. Lu · X. Wang
Materials Chemistry Laboratory, Nanjing University of Science
& Technology, Nanjing 210094, P.R. China

zirconium oxychloride ($\text{ZrOCl}_2 \cdot 8\text{H}_2\text{O}$) and ammonium peroxydisulfate (APS), both of analytical reagent grade, were purchased from the China National Medicine Group Shanghai Chemical Reagent Company; oxalic acid dihydrate ($\text{C}_2\text{H}_2\text{O}_4 \cdot 2\text{H}_2\text{O}$) and absolute ethanol, both of analytical reagent grade, were purchased from Nanjing Chemical Reagent No. 1 Factory, China. Prior to use, MMA was extracted with brine to remove the polymerization inhibitor.

Preparation

First of all, superfine powders of poly (methyl methacrylate) (PMMA) were prepared according to a previous literature report [19]. SDS (0.5 g) was dissolved in distilled water (50 mL) with magnetic stirring, the solution was heated to 80 °C, and then APS (0.25 g) was added. The mixture was stirred to form a homogeneous solution, and then MMA (10 mL) was added dropwise over a period of 1.5–2.0 h, ensuring that the reaction proceeded to completion. Subsequently, the appropriate amount of saturated sodium chloride solution was added to the reaction mixture to obtain the products by destroying the emulsion. The precipitate was centrifuged, washed three times with distilled water, and dried at 60 °C in a vacuum oven. The loose, superfine powders of PMMA were obtained by further grinding of these precipitates.

Superfine PMMA powder (1.0 g) was added to a 0.25 M solution of oxalic acid in ethanol (40 mL) with continuous dispersal under ultrasonic conditions until a white suspension was obtained. This suspension was then slowly added to a 0.5 M solution of zirconium oxychloride in water (20 mL) under magnetic stirring to form a white sol [18]. The sol was left to stand for 24 h so as to form a gel, which was dried at 40 °C and then ground to obtain the white precursor, which was calcined at 500 °C for 1 h to form the mesoporous zirconia. All other experiments were performed at ambient temperature.

Instruments

Specific surface area, pore volume, and pore size distribution of the nanosized mesoporous zirconia were determined from N_2 adsorption–desorption isotherms at 77 K (Micrometrics ASAP 2010). Surface area was calculated using the BET equation; pore volume and pore size distribution were calculated by the BJH method. Prior to the adsorption measurement, samples were degassed under vacuum at 100 °C for 1 h to eliminate any physisorbed moisture. The surface groups were studied by Fourier-transform infrared (FT-IR) microwave spectrophotometry (Bruker Vector22); spectra were recorded in the range 400–4,000 cm^{-1} from samples in KBr pellets.

The crystalline phase and crystallinity of the samples were measured by X-ray powder diffraction (XRD) analysis (Bruker D8 Advance) using Cu-K_α radiation ($\lambda = 0.15406 \text{ nm}$); the samples were scanned over a 2θ range of 0–70° at a scanning rate of 1 degree per minute. The morphology was determined by transmission electron microscopy (TEM) using a JEOL JEM-2100 apparatus.

Results and Discussion

Mechanism of Preparation

Figure 1 shows a schematic diagram of the mechanism of preparation of the mesoporous zirconia. From the flow schematic diagram, it can be seen that the superfine PMMA powder acts as a template. The PMMA particles were dispersed in the solution of oxalic acid in ethanol using ultrasound to form a white suspension, which indicated that the dispersed PMMA particles were in the micron or sub-micron size range. When the PMMA suspension was added to an aqueous solution of zirconium oxychloride, a sol was formed around the PMMA particles (as shown in Fig. 1a). Subsequently, this sol (inlaid with PMMA particles) was left to stand for 24 h so as to form a gel, which was dried at 373 K. Thereafter, the dried gel was ground to obtain gel particles in the micron or submicron size range, with the PMMA particles still embedded in the dried gel particles (as shown in Fig. 1b, c). Finally, the dried gel particles were calcined at 500 °C for 1 h, whereupon the dried gel crystallized into zirconia nanocrystals, while the PMMA particles were concomitantly decomposed into gas which diffused out of the structure, leaving voids and pores in the nanocrystalline zirconia particles. In this procedure, the space initially occupied by the PMMA particles shrinks because of the crystallization of the gel, as a result of which the pore wall collapses from micron or submicron size to the nanosized range. On the basis of the above discussions, it can be concluded that the PMMA particles act as templates in the preparation of the mesoporous zirconia.

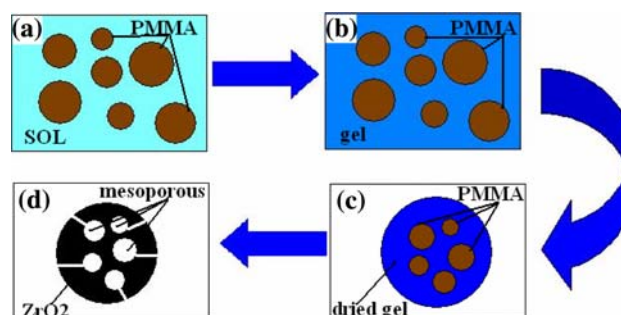


Fig. 1 Schematic diagram of the mechanism of preparation of mesoporous ZrO_2

FT-IR Analysis

Figure 2 shows the FT-IR spectrum of the PMMA. From Fig. 2, it can be seen that there is a distinct absorption band from $1,150\text{ cm}^{-1}$ to $1,250\text{ cm}^{-1}$, which can be attributed to the C–O–C stretching vibration. The two bands at $1,388\text{ cm}^{-1}$ and 754 cm^{-1} can be attributed to the α -methyl group vibrations. The band at 987 cm^{-1} is the characteristic absorption vibration of PMMA, together with the bands at $1,062\text{ cm}^{-1}$ and 843 cm^{-1} . The band at $1,732\text{ cm}^{-1}$ shows the presence of the acrylate carboxyl group. The band at $1,444\text{ cm}^{-1}$ can be attributed to the bending vibration of the C–H bonds of the $-\text{CH}_3$ group. The two bands at $2,997\text{ cm}^{-1}$ and $2,952\text{ cm}^{-1}$ can be assigned to the C–H bond stretching vibrations of the $-\text{CH}_3$ and $-\text{CH}_2-$ groups, respectively. Furthermore, there are two weak absorption bands at $3,437\text{ cm}^{-1}$ and $1,641\text{ cm}^{-1}$, which can be attributed to the $-\text{OH}$ group stretching and bending vibrations, respectively, of physisorbed moisture. On the basis of the above discussions, it can be concluded that the prepared polymer was indeed macromolecular PMMA [20].

Figure 3 shows the FT-IR spectrum of the mesoporous zirconia. There is a strong absorption band at 471 cm^{-1} , which can be attributed to the tetragonal zirconia. Furthermore, there is no characteristic absorption band of monoclinic zirconia. These observations suggest that the products consisted only of tetragonal zirconia. The two bands at $3,419\text{ cm}^{-1}$ and $1,626\text{ cm}^{-1}$ can be attributed to the stretching and bending vibrations of the $-\text{OH}$ groups of the physisorbed moisture [21].

XRD Analysis

Figure 4 displays the XRD pattern of the mesoporous zirconia. There are four strong diffraction peaks at 30.55° ,

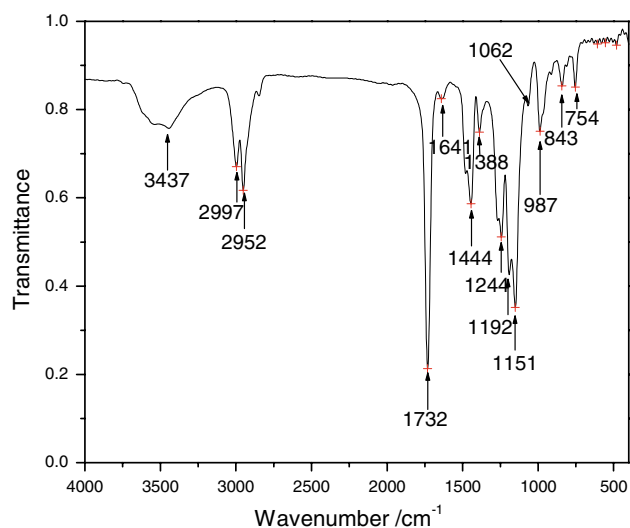


Fig. 2 FT-IR spectrum of PMMA

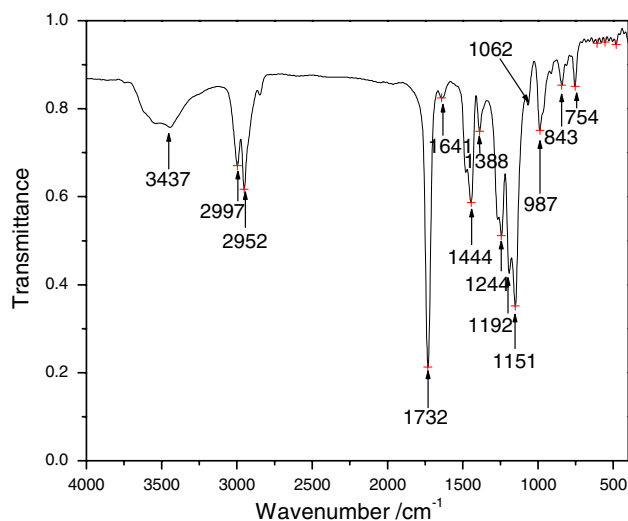


Fig. 3 FT-IR spectrum of the mesoporous ZrO_2

35.40° , 50.70° , and 60.35° , which can be attributed to the (111), (200), (220), and (311) diffraction planes of the tetragonal zirconia by the standard card No.79–1771(Computer searching system). Furthermore, there is no characteristic diffraction peak of monoclinic zirconia, $m\text{-ZrO}_2$, indicating its absence from the products.

Textural Analysis

N_2 adsorption–desorption isotherms of the mesoporous zirconia measured at 77 K are shown in Fig. 5; Fig. 5a relates to the precursor sample and Fig. 5b relates to the product obtained from the precursor sample after calcination at 500°C for 1 h. In Fig. 5a, it may be noted that the adsorption isotherm and desorption isotherm of the precursor have not been enclosed, indicating the absence of a pore structure. However, in Fig. 5b, it may be noted that

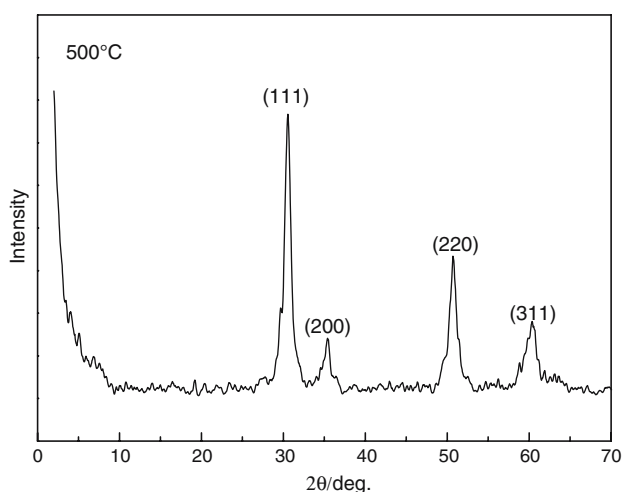


Fig. 4 XRD pattern of the mesoporous ZrO_2

the adsorption isotherm and desorption isotherm of the calcined product are been enclosed, as befits an IUPAC type IV material, suggesting the presence of mesopores [22]. The hysteresis loop observed for the calcined product, between $P/P_0 = 0.35$ and $P/P_0 = 0.90$, is of type H_2 , reflecting the presence of bottle-shaped mesopores on the basis of the Kelvin law [22]. Furthermore, the specific surface area of the mesoporous zirconia is $63.7 \text{ m}^2/\text{g}$, while that of the precursor sample is $30.3 \text{ m}^2/\text{g}$; the corresponding pore volume of the mesoporous sample is $0.07 \text{ cm}^3/\text{g}$, while that of the precursor sample is $0.02 \text{ cm}^3/\text{g}$. These results indicate that the mesoporous structures were generated during calcination of the dried gel, corroborating the mechanism of preparation outlined in Fig. 1.

Figure 6 shows the pore size distribution of the mesoporous ZrO_2 . From Fig. 6, it can be observed that there is only one peak centered at 3.7 nm, suggesting the presence of a uniform pore size. Furthermore, the peak shape is very narrow, indicating that the mesoporous zirconias have a sharply defined pore size distribution. In general, the results of our study of the pore size distribution are consistent with the above-described N_2 adsorption–desorption isotherms.

Figure 7 shows the TEM image of the mesoporous zirconia. From the image, it can be seen that there are many spherical pores. The pore size is in the range of 2–6 nm, and these data are consistent with the results presented in Fig. 6.

Conclusions

Superfine PMMA powders have been prepared using an emulsion polymerization method. Using the PMMA particles thus obtained as templates, and zirconium oxychloride and oxalic acid as raw materials, tetragonal phase mesoporous zirconia has been synthesized using a sol–gel method. FT-IR, XRD, TEM, and N_2 adsorption–desorption isotherms have been used to characterize the products. The results have indicated that the average pore size of

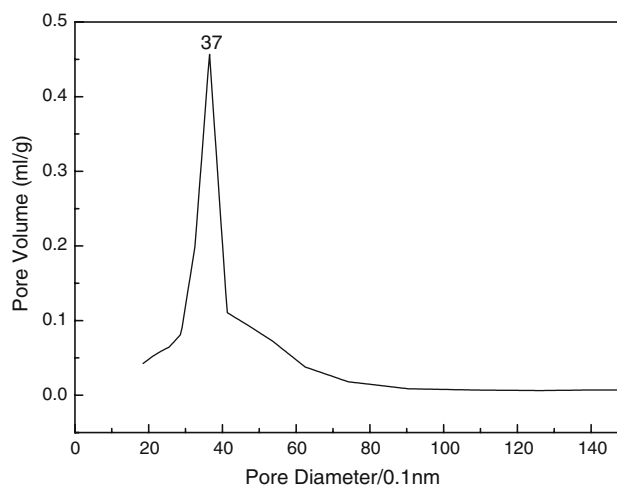


Fig. 6 Pore size distribution of the mesoporous ZrO_2

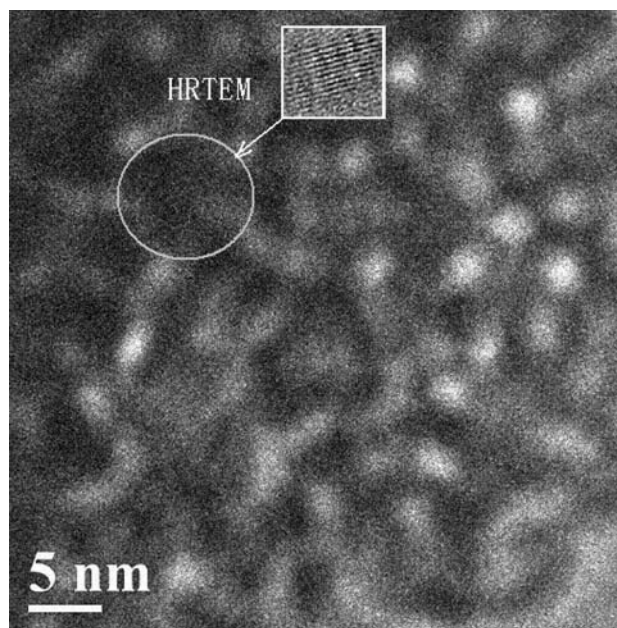
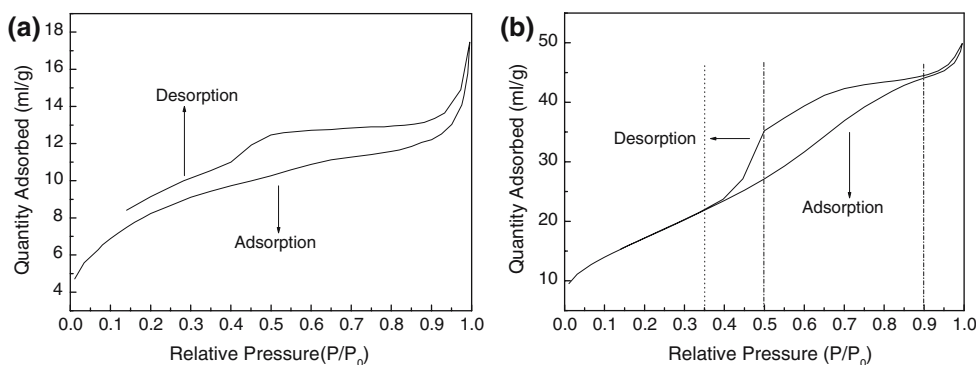


Fig. 7 TEM image of the mesoporous ZrO_2

Fig. 5 N_2 adsorption–desorption isotherms of nanosized ZrO_2



mesoporous zirconia was found to be 3.7 nm, and the pore size distribution was favorably narrow.

Acknowledgment This work was supported by the National Science Foundation of Jiangsu Province, China (Grant No. BK2003097). The authors are grateful for the grant.

References

1. Y.Y. Lyu, S.H. Yi, J.K. Shon, Highly stable mesoporous metal oxides using nano-propping hybrid gemini surfactants. *J. Am. Chem. Soc.* **126**, 2310 (2004)
2. S.Y. Chen, L.Y. Jang, S. Cheng, Synthesis of thermally stable zirconia-based mesoporous materials via a facile post-treatment. *J. Phys. Chem. B* **110**, 11761 (2006)
3. Z.G. Shi, L.Y. Xu, Y.Q. Feng, A new template for the synthesis of porous inorganic oxide monoliths. *J. Non-cryst. Solids* **352**, 4003 (2006)
4. M.S. Wong, J.Y. Ying, Amphiphilic templating of mesostructured zirconium oxide. *Chem. Mater.* **10**, 2067 (1998)
5. S. Sadasivan, G.B. Sukhorukov, Fabrication of hollow multifunctional spheres containing MCM-41 nanoparticles and magnetite nanoparticles using layer-by-layer method. *J. Colloid Interf. Sci.* **304**, 437 (2006)
6. S.B. Yoon, J.Y. Kim, J.H. Kim, Template synthesis of nanostructured silica with hollow core and mesoporous shell structures. *Curr. Appl. Phys.* **6**, 1059 (2006)
7. Z.B. Xu, X.W. Wei, Chin, Preparation and characterization of TiO₂ hollow microspheres. *J. Electron Microsc. Soc.* **25**, 26 (2006)
8. Z.P. Gan, J.G. Guan, Chemical self-assembly route to fabricate hollow barium ferrite submicrospheres. *Acta Phys-Chim. Sin.* **22**, 189 (2006)
9. M. Signoretto, A. Breda, F. Somma, Mesoporous sulphated zirconia by liquid-crystal templating method. *Micropor. Mesopor. Mat.* **91**, 23 (2006)
10. M.A. David, Hollow ordered zirconia microcage formation by spherical micelle templating with chelating triol surfactants. *Micropor. Mesopor. Mat.* **28**, 505 (1999)
11. Y.B. Suo, Y.C. Du, J.X. Zhang, Y.L. Zhang, Synthesis of ZrO₂ mesoporous materials by liquid phase method. *J. Chin. Cer. Soc.* **33**(9), 1081 (2003)
12. V.I. Alexander, S.V. Lysenko, S.V. Baranova, Thermally stable materials based on mesostructured sulfated zirconia. *Micropor. Mesopor. Mat.* **91**, 254 (2006)
13. J. Yin, X.F. Qian, J. Yin, Preparation of polystyrene/zirconia core-shell microspheres and zirconia hollow shells. *Inorg. Chem. Commun.* **6**, 942 (2003)
14. S.J. Ding, C.L. Zhang, M. Yang, Template synthesis of composite hollow spheres using sulfonated polystyrene hollow spheres. *Polymer.* **47**, 8360 (2006)
15. X.M. Liu, G.Q. Lu, Z.F. Yan, Synthesis and stabilization of nanocrystalline zirconia with MSU mesostructure. *J. Phys. Chem. B* **108**, 15523 (2004)
16. G.R. Duan, X.J. Yang, G.H. Huang, Water/span80/ Triton X-100/n-hexyl alcohol/n-octane microemulsion system and the study of its application for preparing nanosized zirconia. *Mater. Lett.* **60**, 1582 (2006)
17. G.R. Duan, X.J. Yang, A.Q. Lu, Comparison study on the high-temperature phase stability of CaO-doped zirconia made using different precipitants. *Mater. Charact.* **58**, 78 (2007)
18. H.X. Xi, Z.T. Huang, Preparation and characterization of zirconia precursor-zirconyl oxalate. *J. Inorg. Mater.* **11**, 547 (1996)
19. L.J. Zhang, J.L. Chen, Z.Y. Zhao, Study on in situ emulsion polymerization of nano-scale TiO₂/methyl methacrylate. *Paint & Coat. Ind.* **33**, 1 (2003)
20. Z.X. Lin, *Analysis and Identification of Infrared Spectrum of the Polymer* (Sichuan University Press, Chengdu, 1989)
21. C.M. Phillippi, K.S. Mazdiyasi, Infrared and Raman spectra of zirconia polymorphs. *J. Am. Ceram. Soc.* **54**, 254 (1997)
22. R.R. Xu, W.Q. Pang, *Molecular Sieve and Multi-pore Material Science* (Science Press, 2004)